Vibrational spectra in ordered and disordered Ni$_3$Al

Jeffrey D. Althoff, Dane Morgan, and Didier de Fontaine

Department of Materials Science and Mineral Engineering, University of California, Berkeley, California 94720

Mark Asta, S. M. Foiles, and D. D. Johnson

Computational Materials Science Department, Sandia National Laboratories, MS 9161, Livermore, California 94551

(Received 18 March 1997)

We calculate the vibrational density of states (DOS) and corresponding thermodynamic properties of $L1_2$ ordered and disordered Ni$_3$Al in the quasiharmonic approximation using the embedded-atom method. Vibrational and thermodynamic properties, including vibrational entropy differences between ordered and disordered states, are found to be in good agreement with experiment. The DOS of the configurationally disordered alloy resembles a broadened version of the DOS of the $L1_2$ phase, not a one-atom per cell fcc DOS, and is shifted downward in frequency because the disordered state has a larger volume than the ordered phase. Calculations of the projected DOS indicate that high-frequency modes located predominantly on aluminum atoms broaden the most on disordering. Further, we find that the vibrational entropy difference between the two phases is largely due to the difference in volumes of the phases and their different thermal expansions. [S0163-1829(97)51334-8]

Recent measurements[1,2] on ordered and disordered alloys suggest that in some systems the vibrational contribution to the entropy difference between ordered and disordered phases may be a sizable fraction of the total entropy difference. This suggests that an understanding of the thermodynamics of alloys, and their temperature-composition phase diagrams, requires consideration of both vibrational and configurational entropic contributions. A well-studied example is the technologically important Ni$_3$Al compound, which possesses the $L1_2$ structure, a superstructure of fcc. The corresponding fcc disordered phase does not exist at equilibrium, but has been prepared experimentally by laser quenching,[3] vapor deposition onto cold substrates,[1] and by mechanical alloying.[2,4] Specific heat measurements[1] up to 343 K indicate a vibrational entropy difference $\Delta S_{\text{vib}} = S_{\text{dis}} - S_{L1_2}$ of at least $+0.19k_B$ per atom; an extrapolation[1] based on the Debye model gives $\Delta S_{\text{vib}} = +0.27k_B$ per atom at 1700 K. Extended electron energy-loss fine structure spectroscopy measurements[1] give a similarly large vibrational entropy excess for the disordered state. Inelastic neutron scattering measurements[2] likewise give a large result: $\Delta S_{\text{vib}} = 0.2 \pm 0.1k_B$ per atom.

It has been proposed by Fultz *et al.*[2] that this large vibrational entropy difference is due to a change in the character of the vibrational spectrum associated with chemical disordering of the system: the $L1_2$ compound has a light and stiffly bonded aluminum sublattice leading to high-frequency modes which lower the vibrational entropy of the ordered alloy. In contrast to the explanation of Fultz *et al.*,[2] Ackland[5] demonstrated through calculations based on "many-body" potentials that the entropy difference arises primarily from the larger volume of the disordered phase relative to the ordered phase. Ravelo *et al.*,[6] using molecular dynamics simulations, also find a large vibrational entropy difference that they trace to the volume difference between the phases. The purpose of the present work is to understand, through a de-

tailed analysis of the vibrational spectra, how disorder and volume effects separately influence the vibrational properties of alloys, with Ni$_3$Al as the test case.

We find that, at fixed volume, the effect of disorder is to broaden the vibrational DOS of the disordered phase relative to that of the ordered $L1_2$ phase. The exact nature of the changes in the vibrational spectra, especially related to specific environmental effects, are detailed below. The dominant feature affecting the entropy difference is the larger equilibrium volume of the disordered phase which "contracts" the disordered DOS, thereby shifting spectral weight to lower frequencies relative to the disordered DOS at the equilibrium volume of the $L1_2$ phase. Changes in the phonon spectrum associated with the chemical disorder at fixed lattice constant account for only about 20% of the observed vibrational entropy difference. Therefore, the change in character of the phonon spectrum, as proposed by Fultz *et al.*,[2] is not the largest factor contributing to the large entropy difference. The bulk of the vibrational entropy difference arises from the difference in volume between the ordered and disordered phases. This equation of state (EOS) effect is of course influenced by the change in phonon spectra, but it also has a component that is determined by zero-temperature considerations.

We perform calculations of the vibrational spectra and thermodynamic properties of $L1_2$-ordered and completely disordered (no short-range-order) Ni$_3$Al in the quasiharmonic approximation[7] using embedded-atom method[8,9] (EAM) potentials. The specific potentials used here were developed by Voter and Chen[10] for Ni$_3$Al. These EAM functions are fit to the lattice constants, cohesive energies, bulk moduli, elastic constants, vacancy formation energies, and the bond length and bond energy of the diatomic molecules of elemental Ni and Al, as well as to the lattice constant, cohesive energy, elastic constants, vacancy formation energy, super intrinsic stacking fault energy, and (100) and (111) antiphase boundary energies of Ni$_3$Al, and to the lat-

tice constant and cohesive energy of the $B2$ phase of NiAl. No temperature dependence of the parameters was used in the fit.

Within the quasiharmonic approximation,[7] the phonon frequencies are functions of the volume, and the equilibrium volume is that which minimizes the Gibbs free energy at a given pressure. In practice, we calculate the vibrational spectra over a range of volumes and perform sums over the first Brillouin zone to obtain, for example, the Helmholtz free energy

$$F = k_B T \sum_{j\vec{k}} \ln\left[2 \sinh\left(\frac{\hbar \omega_j(\vec{k};V)}{2 k_B T} \right) \right] \qquad (1)$$

as a function of volume V and temperature T. One can then calculate the pressure $P = -(\partial F/\partial V)_T$ and find the volume $V(T,P)$ which minimizes the Gibbs energy $G = F + PV$ at the desired pressure P. In the present work, we are concerned with the zero pressure EOS. We compute the vibrational entropy S and the specific heat at constant volume c_V directly by summing the appropriate functions over the vibrational spectra. The vibrational spectra themselves are obtained by diagonalizing the dynamical matrices for the structure of interest at the desired volume. The specific heat at constant pressure is obtained from the thermodynamic relation $c_P = c_V + TVB\beta^2$, where $V(T)$ is the equilibrium volume at temperature T, $B(T)$ is the isothermal bulk modulus, and $\beta(T)$ is the (volume) thermal expansion coefficient. $\beta(T)$ is obtained from the relation $\beta B = (\partial S/\partial V)_T$. Once the EOS for a phase is in hand, one can examine the DOS at a volume appropriate for the temperature under consideration.

To treat the disordered phase, we generate an initial lattice of 256 randomly occupied sites with stoichiometry Ni_3Al. We apply periodic boundary conditions. We relax the structure using conjugate-gradient energy minimization, then compute its vibrational spectrum by diagonalizing the dynamical matrix at many points in the Brillouin zone. We obtain thermodynamic properties using the quasiharmonic approximation as outlined above. The vibrational DOS for either phase is obtained at the desired volume by calculating the spectra over many points in the Brillouin zone and counting modes. To obtain the DOS for the disordered phase, we average over 10 disordered configurations—a similar averaging technique was used by Rubini and Ballone[11] in their work on phonon localization in the Ni-Al system. Internal relaxation typically changes the vibrational entropy of the disordered phase by about 1%, leading to a decrease in ΔS_{vib} of approximately 20%. Averaging over 20 disordered configurations to calculate, e.g., the vibrational entropy, leads to a standard deviation that is much less than 1% of the value of the vibrational entropy itself—this translates into a standard deviation of approximately 1% for the vibrational entropy difference between ordered and disordered states. Increasing the number of atoms in the disordered configuration to 500 does not change the results appreciably. For any specific disordered configuration, all sums over the spectra are converged with respect to the number of $\vec{k}$ points to an uncertainty that is smaller than any associated with averaging over disordered configurations. We typically use 64 $\vec{k}$ points for calculating thermodynamic quantities, and as many as 1000 for calculating the DOS. We mention that we have not
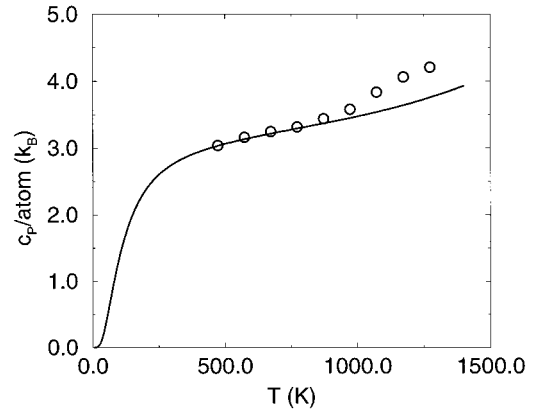

FIG. 1. Specific heat at constant pressure (per atom, in units of Boltzmann's constant) for the ordered $L1_2$ phase of Ni_3Al. The solid line is the calculation, and the symbols are data from Ref. 14.

elected to pursue a calculation based on an approximation to the configurational averaging, such as the coherent potential approximation[12] (CPA), for two reasons. The first reason is that the CPA has difficulty reproducing the results of exact diagonalizations[12,13] (against which the CPA was benchmarked[12]) for light-mass defect systems. The second reason is that it is necessary to assess the effect of local relaxations on the phonon spectrum, a problem that the CPA, as currently formulated, seems ill equipped to address. Cruder models of disorder such as the virtual crystal approximation (which is still invoked to interpret experimental data) are even less valid, especially for investigating the DOS.

To investigate the validity of the quasiharmonic model and of the EAM potential employed, we calculate a variety of thermodynamic quantities. In Fig. 1 we show the vibrational contribution to $c_P(T)$ for $L1_2$ Ni_3Al compared to experimental data.[14] Agreement is remarkably good over the temperature range for which vibrational effects alone are expected to contribute. Calculations of antisite defect energies[15] reveal that the deviation from experiment of $c_P(T)$ coincides with the onset of the production of significant numbers of equilibrium antisite defects. Thus, above approximately 900 K, the experimentally measured c_P (open circles) begins to deviate from the calculated vibrational c_P curve. We find a temperature-dependent ΔS_{vib} equal to $0.11k_B$ at 600 K, $0.15k_B$ at 1000 K, and 0.27 at 1400 K. This is consistent with the experimental thermodynamic measurements.[1] The quasiharmonic results for $V(T)$ for ordered and disordered phases show that the equilibrium volumes of the two phases differ by about 1% at zero temperature and by about 2% at 1000 K. The corresponding lattice constant difference is about 0.4% at 300 K and approximately 0.6% at 1000 K, which is consistent with the experimental results of Cardellini *et al.*[4] and with the theoretical results of Wolverton,[16] Johnson,[17] and Ravelo *et al.*[6] but not with the most recent results of Fultz.[18] We take all these results as an indication that the thermodynamic model used here is reasonable.

In discussing the vibrational entropy difference between the disordered and ordered phases, it is useful to exploit the thermodynamic relationship between c_P and c_V and write
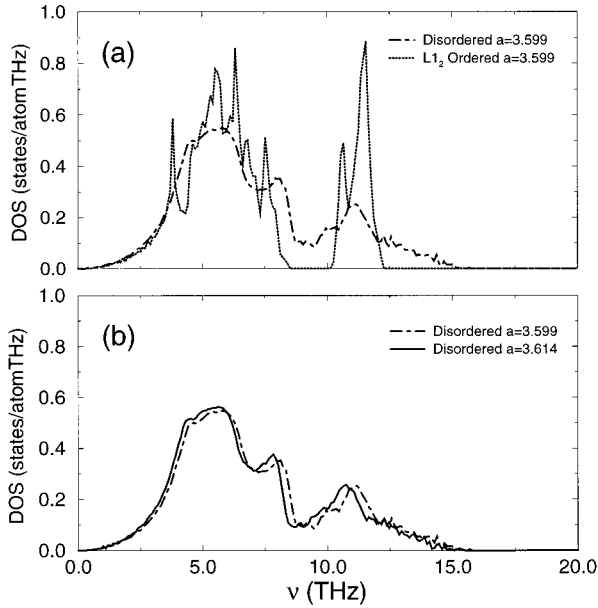
FIG. 2. (a) Vibrational DOS for $L1_2$ ordered (dotted curve) and disordered Ni_3Al (dot-dashed curve), both calculated at the equilibrium lattice constant for the $L1_2$ phase. (b) Vibrational DOS for the disordered phase at two different lattice constants. The solid curve is the DOS for disordered Ni_3Al at its equilibrium lattice constant corresponding to $T = 400$ K. The dot-dashed curve is the DOS for disordered Ni_3Al at the lattice constant appropriate to the ordered $L1_2$ phase at $T = 400$ K.

$$\Delta S_{\text{vib}}(T) = \int_0^T \frac{\Delta c_V}{T'} dT' + \int_0^T \Delta(V B_T \beta^2) dT'. \qquad (2)$$

The first term in Eq. (2) tends to a constant for temperatures $T > \theta_D$, the Debye temperature; the second term leads to an approximately linear temperature dependence for ΔS_{vib} that can be appreciable if, for example, the equations of state of the two phases are considerably different. As discussed in the previous paragraph, the volumes of the two phases differ considerably throughout the temperature range, as do the thermal expansions. This is the dominant contributing factor to the large value of ΔS_{vib} seen here.

In Fig. 2(a) we show the vibrational DOS of the $L1_2$ phase at its lattice constant at $T = 400$ K and the vibrational DOS of the disordered state at the same lattice constant. In Fig. 2(b) we show the vibrational DOS of the disordered state at the equilibrium volumes of the ordered phase and the disordered phase both at 400 K. Both disordered vibrational DOS curves were obtained by averaging over 10 different disordered configurations. The ordered DOS is in good agreement with the measurements of Stassis *et al.*[19] The main difference is that the gap between the low- and high-frequency portions of the spectra is about 1 THz too large. A comparison of the two DOS in Fig. 2(a) shows that, at fixed volume, the DOS of the disordered state resembles a broadened version of the $L1_2$ DOS. In particular, it does not resemble the DOS for a monatomic fcc metal, thereby casting serious doubt on the use of the virtual crystal approximation in analyzing diffraction data from disordered samples. In Fig. 2(b), the effect of the change in volume is evident: the larger volume of the disordered phase shifts its vibrational
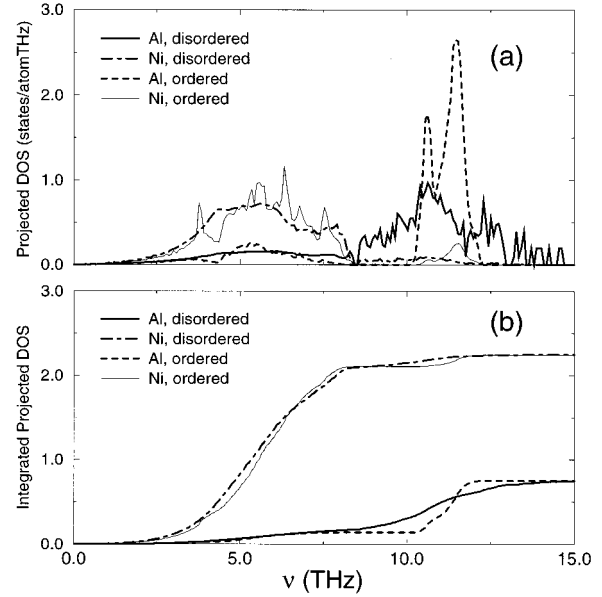
FIG. 3. (a) Projected phonon DOS for $L1_2$ ordered and disordered Ni_3Al. The dashed curve is the Ni-projected DOS for disordered Ni_3Al at its equilibrium lattice constant corresponding to $T = 400$ K. The heavy solid curve is the Al-projected DOS for disordered Ni_3Al at its equilibrium lattice constant corresponding to $T = 400$ K. The light solid curve is the Ni-projected DOS for $L1_2$ ordered Ni_3Al at its equilibrium lattice constant corresponding to $T = 400$ K. The dotted curve is the Al-projected DOS for $L1_2$ ordered Ni_3Al at its equilibrium lattice constant corresponding to $T = 400$ K. (b) Integrated projected phonon DOS for $L1_2$ ordered and disordered Ni_3Al. The line styles have the same meaning as in the bottom panel.

DOS downward relative to what it would be if it had the same lattice constant as the $L1_2$ phase. This shift accounts for about 80% of the entropy difference between ordered and disordered states.

To investigate in more detail the nature of the broadening due to configurational disorder, in Fig. 3(a) we show the DOS projected onto Ni and Al atoms in the ordered and disordered state. The narrow peak in the Al-projected DOS in the ordered structure has been identified[2] as being due to a ''sublattice of stiffly bonded, light aluminum atoms in the $L1_2$ structure'' and has been hypothesized[2] to cause the lower vibrational entropy of the ordered state. We find that the splitting of the high-frequency peak from the rest of the spectrum is largely controlled by the mass difference between Ni and Al. A model calculation, in which the masses of Ni and Al were artificially made equal, shows no split-off high-frequency peak at all. From Fig. 3(a), it is clear that the states of the narrow, high-frequency peak in the $L1_2$ structure (which are predominantly of Al character) are significantly more broadened than, for example, the predominantly Ni states at lower frequency. In this context, it is not at all surprising that vibrational intensity is found[2] in the disordered alloy in the frequency range where the high-frequency optical peak is found in the ordered alloy—it is a natural consequence of the broadening. Figure 3(b) shows the integrated projected DOS curves corresponding to Fig. 3(a). The downward shift caused by volume relaxation of the disordered phase is again evident for both the Ni and Al states.

The fact that the Al states are more affected by the configurational disorder can be rationalized by a simple nearest-neighbor bond counting argument. In the $L1_2$ state, the Al is surrounded by 12 heavier Ni atoms and the Ni atoms have eight Ni neighbors. For the disordered state, on average, both Al and Ni have nine Ni neighbors. Thus the local environment of the Al atoms is more greatly affected. Furthermore, the introduction of lighter aluminum first neighbors in the disordered alloy leads to localized modes split off from the high-frequency end of the spectrum. Calculations of the inverse participation ratio in the disordered alloy show that the high-frequency modes (at frequencies above those of the $L1_2$ optical peak in the ordered alloy), as are evident in Fig. 3(a), are localized predominantly on groups of 20 or fewer Al atoms. Similarly, in the $L1_2$ structure, Al has only Al second neighbors. The introduction of heavier Ni second neighbors in the disordered alloy can further broaden the $L1_2$ structure's optical peak. The introduction of heavy second neighbors is expected to broaden the high-frequency peak towards lower frequencies, similar to the existence of low-frequency resonant modes in heavy impurity systems.[20] A model calculation on an $L1_2$ supercell in which a Ni atom is swapped with a (distant) Al atom shows this behavior. The spectra reveal modes split off from the $L1_2$ structure's optical peak, one set of modes that are predominantly on Al atoms split off to high frequency, and one set of modes that have some Ni character split off to low frequency. Such local environment effects cannot be described within simple models (such as the CPA or the virtual crystal approximation), whereas our direct approach provides complete information.

In conclusion, our detailed analysis of the vibrational spectra and thermodynamics of the ordered $L1_2$ and disordered phases of Ni_3Al showed that, while there is an interesting rearrangement of the phonon spectrum upon disordering, the bulk of the vibrational entropy difference can be traced to the volume difference between the two phases. Furthermore, the behavior of the vibrational spectrum upon disordering can be understood from simple qualitative arguments based on a mass defect picture. We also conclude that internal relaxations reduce the value of ΔS_{vib} by approximately 20%. Detailed calculations showed that the disordered DOS looks like a broadened $L1_2$ DOS, and that the broadening occurs primarily in the modes associated with Al atoms. The disordered DOS is not well represented by a single atom fcc DOS, which suggests that the virtual crystal approximation is an incorrect way to analyze the vibrational spectrum of the disordered phase. Disorder broadening of the phonon spectrum at fixed lattice accounts for approximately 20% of the observed vibrational entropy difference; the remaining vibrational entropy difference can be traced to the volume difference between ordered and disordered phases.

[1] L. Anthony, J. K. Okamoto, and B. Fultz, Phys. Rev. Lett. **70**, 1128 (1993).

[2] B. Fultz *et al.*, Phys. Rev. B **52**, 3315 (1995).

[3] J. A. West, J. T. Manos, and M. J. Aziz, in *High Temperature Ordered Intermetallic Alloys IV*, edited by L. Johnson, D. P. Pope, and J. O. Stiegler, MRS Symposia Proceedings No. 213 (Materials Research Society, Pittsburgh, 1991), p. 859.

[4] F. Cardellini *et al.*, J. Mater. Res. **8**, 2504 (1993).

[5] Graeme J. Ackland, in *Alloy Modeling and Design*, edited by G. Stocks and P. Turchi (The Minerals, Metals, and Materials Society, Warrendale, PA, 1994), p. 149.

[6] R. Ravelo *et al.* (unpublished).

[7] A. A. Maradudin, E. W. Montroll, G. H. Weiss, and I. P. Ipatova, *Theory of Lattice Dynamics in the Harmonic Approximation*, 2nd ed. (Academic Press, New York, 1971).

[8] Murray S. Daw and M. I. Baskes, Phys. Rev. B **29**, 6443 (1984).

[9] Murray S. Daw, S. M. Foiles, and M. I. Baskes, Mater. Sci. Rep. **9**, 251 (1993).

[10] Arthur F. Voter and Shao Ping Chen, in *Characterization of Defects in Materials*, edited by R. W. Siegel, J. R. Weertman, and R. Sinclair, MRS Symposia No. 82 (Materials Research Society, Pittsburgh, 1988), p. 175.

[11] Silvia Rubini and Pietro Ballone, Phys. Rev. B **50**, 1297 (1994).

[12] D. W. Taylor, Phys. Rev. **156**, 1017 (1967).

[13] Daniel N. Payton III and William M. Visscher, Phys. Rev. **154**, 802 (1967).

[14] A. I. Kovalev, M. B. Bronfin, Yu V. Loshchinin, and V. A. Vertogradskii, High Temp.-High Press. **8**, 581 (1976).

[15] S. M. Foiles and M. S. Daw, J. Mater. Res. **2**, 5 (1987).

[16] C. M. Wolverton (unpublished).

[17] D. D. Johnson (unpublished).

[18] B. Fultz (unpublished).

[19] C. Stassis, F. X. Kayser, C.-K. Loong, and D. Arch, Phys. Rev. B **24**, 3048 (1981).

[20] P. Dean, Rev. Mod. Phys. **44**, 127 (1972).